PHYSOR 2004 -The Physics of Fuel Cycles and Advanced Nuclear Systems: Global Developments
Chicago, Illinois, April 25-29, 2004, on CD-ROM, American Nuclear Society, Lagrange Park, IL. (2004)

Scattering Law Data for Graphite in Gas Cooled High Temperature Reactors

Wolfgang Bernnat*, Jürgen Keinert, Margarete Mattes
Institute for Nuclear Energy and Energy Systems, Pfaffenwaldring 31, D-70550 Stuttgart, Germany

For polycrystalline graphite the presently available scattering law data were re-evaluated to prove their actuality for application of gas cooled reactor studies. Several frequency distributions $\rho(\omega)$ were considered published by Hawari et. al. (NCSU), Nicklow et al. (recently processed by Difilippo et al., ORNL) and Young, Koppel (GA). To get numerical accurate results care was taken to have a correlation of the alpha and beta grid to the maxima and minima of $\rho(\omega)$. The generated scattering law data were used as basis for the calculation of differential and integral neutron cross sections which could be compared with corresponding experimental data. For all investigated models the results agree well with measurements but the overall agreement of the Young, Koppel model (GA) seems to be slightly better than the NCSU and the ORNL model. Especially, the GA model reproduces well the measured cross sections and specific heat data.

The generated data sets were then used to calculate thermal neutron spectra and integral data for different configurations with graphite as moderator. The measured neutron flux spectra in poisoned graphite were sufficiently reproduced by all models. In pure graphite there are some differences in the maximum, the ORNL data result in a slightly harder spectrum compared to IKE/GA and NCSU data and experimental values. However, integral parameters such as k_{eff} for UOX, MOX and ThOX fuel show no significant sensitivity of the regarded scattering law models.

KEYWORDS: graphite, scattering law data S(α,β,T), frequency distributions, thermal neutron cross section, gas cooled reactors

1. Introduction

Solid reactor grade graphite is polycrystalline with a hexagonal lattice structure. This lattice structure is anisotropic due to the hexagonal basal planes which are only weakly coupled. The generation of scattering law data S(α,β,T) in ENDF-6 format [1] with the code LEAPR of the modular nuclear data processing system NJOY-99 [2] or GASKET2 [3] require a generalised isotropic frequency distribution $\rho(\omega)$. An isotropic frequency distribution $\rho(\omega)$ can be derived from a general tensor force dynamical model of the unit cells. In the past this was done by Yoshimori, Kitano [4] and later improved by Young, Koppel [5] (in the following called GA model) by the bond-bending and bond-stretching model in adjusting the used force constants to known compressibility and specific heat data. The anisotropy causes phonon spectra for perpendicular and parallel vibrations of the graphite lattice. Therefore, Young and Koppel have averaged the two parts in Gaussian approximation taking 2/3 of the parallel and 1/3 of the perpendicular part. This isotropic distribution was compiled by GA in the so-called *kernel book* [6] and used as basis for the scattering law data in JEF-2 [7] and ENDF/B-VI [8].

* Corresponding author, Tel. +49-711-685-2118, FAX +49-711-685-2010, E-mail: bernnat@ike.uni-stuttgart.de

Alternatively, a general tensor force model was examined by Nicklow et al. [9] calling it axially symmetric model and considering C-atoms up to the fourth-nearest neighbours. This model results in an isotropic averaged phonon spectrum of the graphite crystal and was used recently by Difilippo et al. [10] (in the following called the ORNL model). In addition to the GA model we processed thermal neutron scattering data also for the ORNL model using the same criteria in generating the α and β grid as for the GA model. Recently Hawari et al. [11] published a new frequency distribution $\rho(\omega)$ (in the following called NCSU) of polycrystalline graphite based on the central force dynamical theory with ab initio 32 atoms of the hexagonal graphite lattice. For these three different frequency distributions we generated scattering law data sets for a number of temperatures and performed comparisons with experimental data and benchmarks.

2. Comparisons of neutron cross sections derived from different frequency distributions

The investigated frequency distributions $\rho(\omega)$ can be seen in Figure 1. Due to the complicated derivation from the dispersion relations all curves show a strong peak structure.

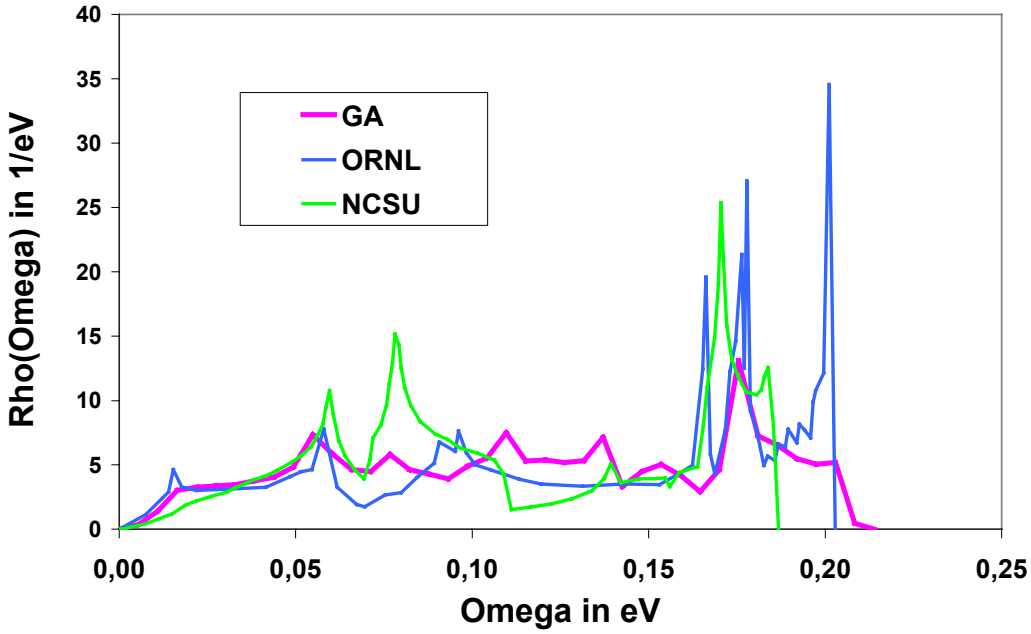

Fig. 1 Frequency distributions of polycrystalline graphite

Whereas the GA model of Young, Koppel is composed of corresponding frequency distributions perpendicular and parallel to the basal hexagonal plane, the ORNL model is derived directly for the theoretical treatment of the anisotropic crystal. For the NCSU model no detailed informations were available. But it is obvious that all frequency distributions are strongly influenced by the choice of the force constants. Especially Young and Koppel have carefully chosen these to get optimal agreement with measured specific heat constants from room temperature up to some hundred degrees of Kelvin.

To evaluate the chosen frequency distributions physical parameters which are directly correlated to $\rho(\omega)$ were regarded such as

- **the specific heat relation** $\frac{C_V}{3R} = \int_0^{\omega_{max}} \left(\frac{\omega}{T}\right) \frac{e^{\omega/T}}{\left(e^{\omega/T}-1\right)^2} \rho(\omega) d\omega$

- **the effective scattering temperature** $T_{eff} = \frac{1}{2} \int_0^{\omega_{max}} \omega \coth \frac{\omega}{2T} \rho(\omega) d\omega$

  3/2 T_{eff} is the average kinetic energy of the system of scattering nuclei. T_{eff} is used to supplement the finite α and β grid of the scattering law data file to higher values of energy and momentum transfers according to the short collision time approximation.

- **the Debye-Waller integral** $\gamma(0) = \int_0^{\omega_{max}} \frac{\rho(\omega)}{\omega} \coth \frac{\omega}{2T} d\omega$

  The Debye-Waller integral is used for calculating the elastic coherent and incoherent thermal neutron scattering cross sections. For coherent scattering the Debye-Waller factor describes the height of the cross sections at the Bragg edges and the exponential decrease between them. Also from the Debye-Waller integral the average and maximal atomic dislocations can be derived ($<u^2> \sim \gamma(0)$).

In Figure 2 the calculated specific heat data for the different generalised frequency distributions together with experimental data [12,13] are shown.

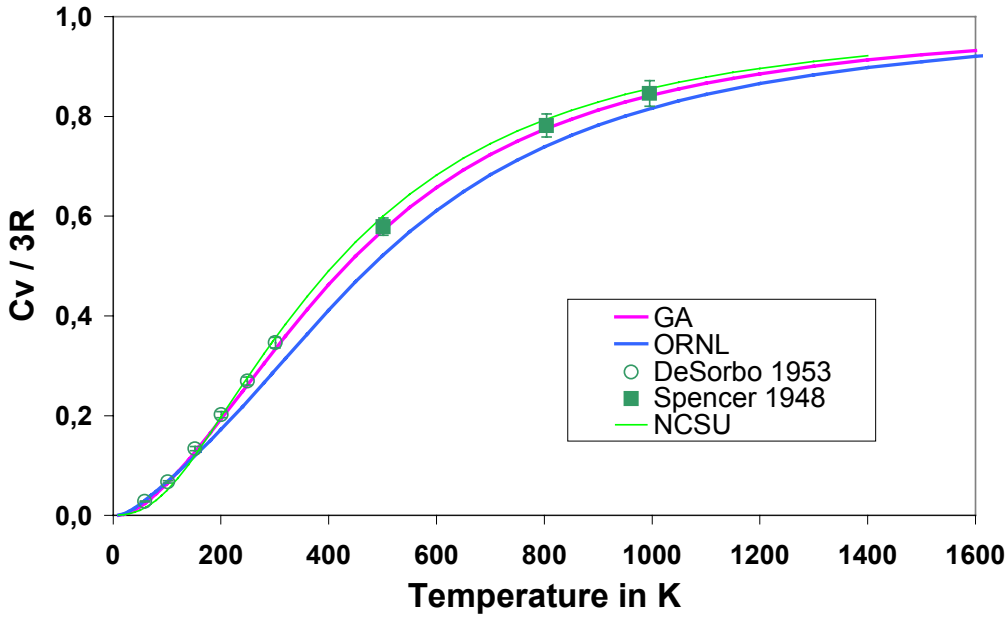

Fig. 2 Specific heat for polycrystalline graphite

As it is clearly seen the specific heat data derived from the ORNL model shows generally too low values, whereas the GA model of Young, Koppel and the NCSU model agree well with the measurements. Further important parameters which are correlated to the frequency distribution are given for room temperature (293.6 K) in Table 1.

For validation of the evaluated Scattering Law Data files S(α,β,T) based on the GA, ORNL and NCSU models measured double differential scattering cross sections of Whittemore [14] for 293 K and for 533 K of Carvalho [15] were compared with corresponding calculated

values.

Table 1 Parameters derived from ρ(ω) for the GA, ORNL and NCSU models for 293 K

Parameter	GA	ORNL	NCSU
$<\omega>/T$	4.596	5.042	4.368
T_{eff}/T	2.43	2.64	2.32
$<\omega^2>/T^2$	25.81	30.67	23.12
$T \bullet \gamma(0)$	0.6586	0.7708	0.5905
<u> in Å	0.067	0.073	0.064

In the Figures 3 to 5 comparisons for room temperature are shown. Figure 3 shows the Scattering Law S(α) for β=2 which describes an energy transfer of 51.7 meV. Following the conservation of energy this is correlated to the first peak region of the phonon spectra. Compared to the measured data the ORNL model seems to underestimate slightly the experiment in this energy region. Figure 4 shows the comparison for β=4 for an energy exchange of 103.4 meV. In this region all investigated models are well within the accuracy of measurement. This energy transfer is correlated to the second peak structure in the frequency distribution ρ(ω).

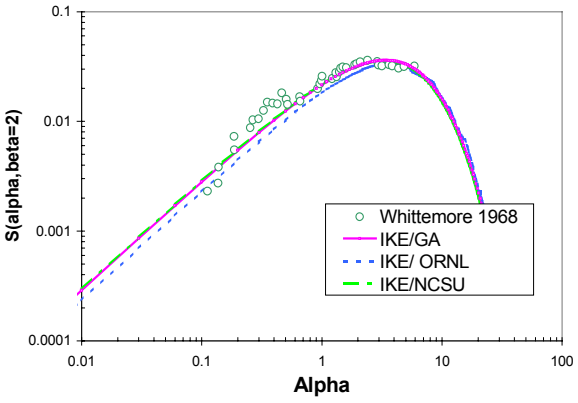

Fig. 3 Graphite Scattering Law for β=2

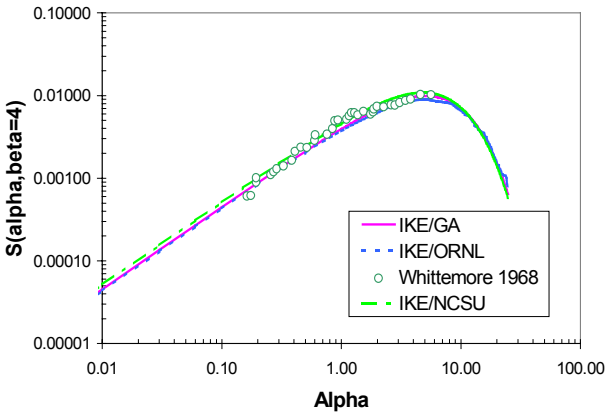

Fig. 4 Graphite Scattering Law for β=4

In Figure 5 the double differential scattering cross section for an initial neutron energy of 325 meV and a scattering angle of 120 degrees is shown. As on the abscissa the transferred energy is given the peaks in the cross sections are directly correlated to the peak structure of the frequency distribution according to the conservation of energy.

Assuming that the published inaccuracy of measurement in Figure 5 is correct it is clearly seen, that the cross sections caused by the peak energies in ρ(ω) are strongly overestimated more or less for all three models. The best agreement is observed for the GA data set. The large peaks in ρ(ω) between 50 meV and 100 meV as well as for 170 meV of the NCSU model are not confirmed by these measurements. For the ORNL model the same observation was made for the large peak around 200 meV.

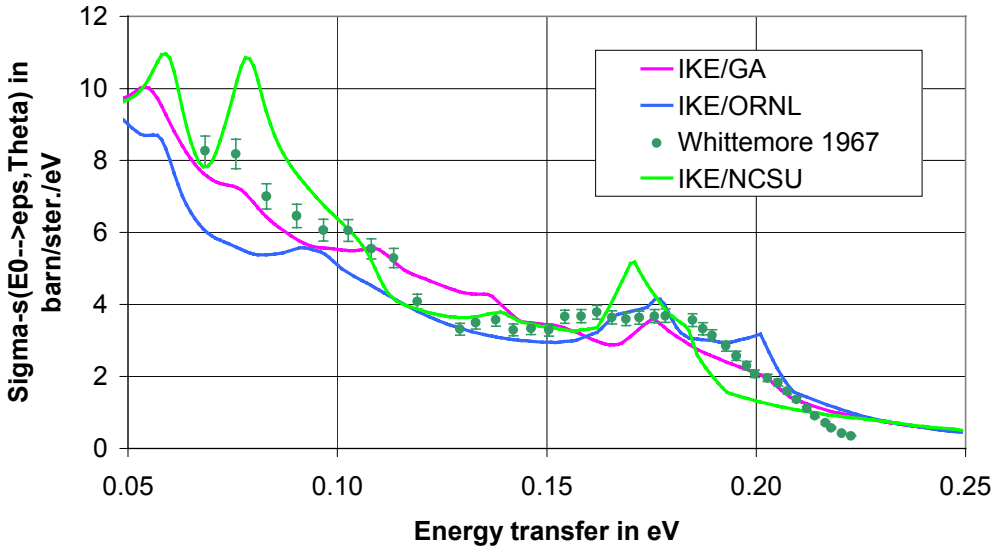

Fig.5 Double differential neutron scattering cross section of graphite (T=293 K)

Generally, for all models of ρ(ω) the weights of the peak structure seem to be overestimated. Their shape should be damped in favour of other energy regions. The best balance over the complete energy range is apparently achieved by the GA model, however.

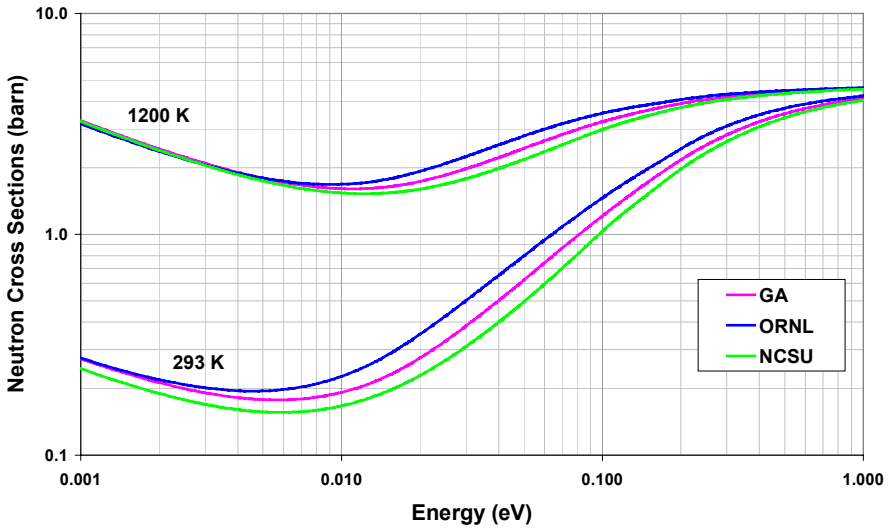

Fig.6 Incoherent inelastic neutron cross sections for graphite

In Figure 6 the incoherent inelastic scattering cross sections for the three models are compared for two temperatures. There are remarkable differences between the investigated models, however this is not of important consequence for the total neutron cross section as the dominating coherent part compensates these effects (due to the different γ(0) for ORNL and NCSU model) as it is seen in Figure 7. Comparing the calculated cross sections with experimental data [16-18] one can see a good agreement over the whole energy range. The discrepancies below .01 meV probably are due to impurities in the measured graphite sample.

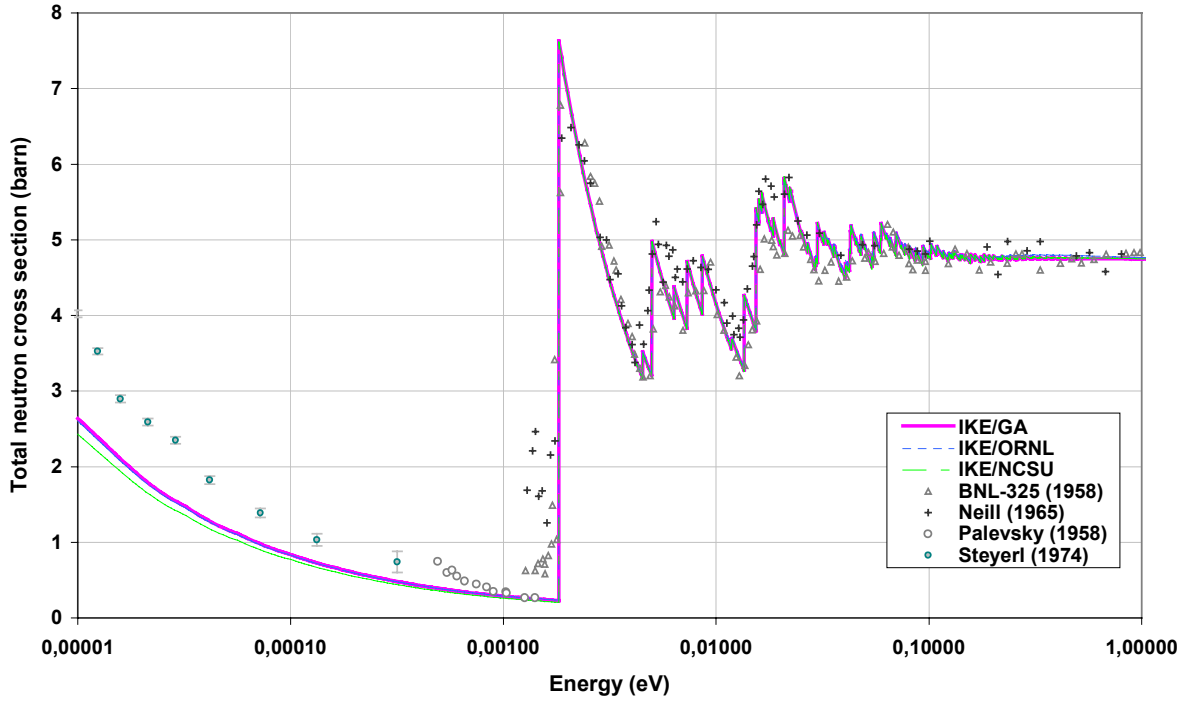

Fig.7 Total neutron cross section of polycrystalline graphite for room temperature

3. Neutron flux density spectra for GA graphite benchmarks

For neutron transport studies in polycrystalline reactor grade graphite cross section data sets for deterministic multigroup and continuous Monte Carlo calculations with MCNP-4C3 were generated with the THERMR, GROUPR and ACER modules of NJOY. The benchmarks are taken from [19]. All measured graphite spectra of [19] for pure and poisoned graphite at different temperatures were calculated with MCNP-4C3 based on the data processed for the three frequency distributions. For some of the experiments a deterministic B_3-method with 292 (127 thermal) energy groups was used. A result is shown in Figure 8 for the experiments GAC-5A and 5F respectively (MCNP-4C3 results). These experiments are composed of two graphite blocks with 274K and 600K separated by a carbon felt. The 274K block was unpoisoned, the 600K block boron poisoned. The thermal neutron spectrum was measured by re-entrance holes in both blocks (GAC-5A 274K, GAC-5F 600K). Figure 8 shows that for the pure graphite at 274 K the calculated (MCNP-4C3) spectra are lower in the maximum compared to the experimental data for all three data models. However, the ORNL model shows a tendency to a harder spectrum. For the spectrum in the poisoned heated graphite block the agreement of the theoretical data and the measurement is better than for the pure graphite. Due to the much harder spectrum the slight differences in the scattering data for the three models are obviously less important. Similar results could also achieved with deterministic calculations.

4. Multiplying systems with graphite as moderator

To investigate the effect of the different scattering data for graphite we analysed thermal systems with different fuel, e.g. $^{233}UO_2$-ThO_2 and highly enriched $^{235}UO_2$ in graphite [20], UO_2 coated particles in HTR pebble bed fuel as well as PuO_2 particles [21] for different

moderator temperatures and moderation ratios. For the temperatures 293 K and 1023 K the data sets based on the GA and the ORNL model resulted in practical identical infinite medium multiplication factors for the $^{233}UO_2$-ThO_2 system [20]. The agreement with the experimental values is quite good. The differences are 0.25 % for room temperature and 0.06 % for 1023 K and may be caused by an unknown content of parasitic absorbers in the graphite and further uncertainties. For the graphite moderated ^{235}U-system the calculated k_∞ values also agree completely for the two thermal neutron graphite data sets at room temperature as well as for 1023 K.

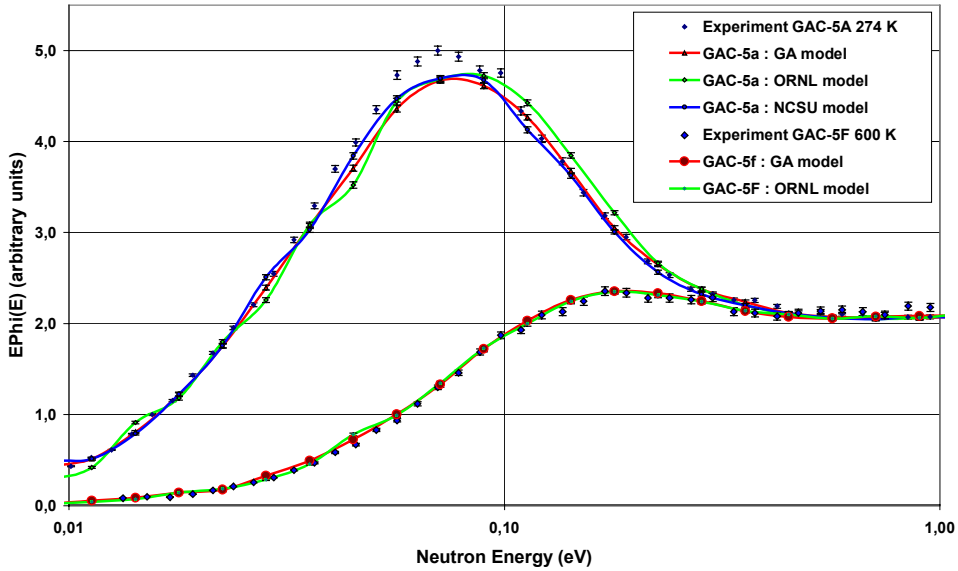

Fig.8 Neutron spectra for the graphite Benchmark GAC-5A and GAC-5F

For infinite lattice HTR pebbles with coated UO_2 particles with different heavy metal content and moderator temperatures the results for the GA model and ORNL model show

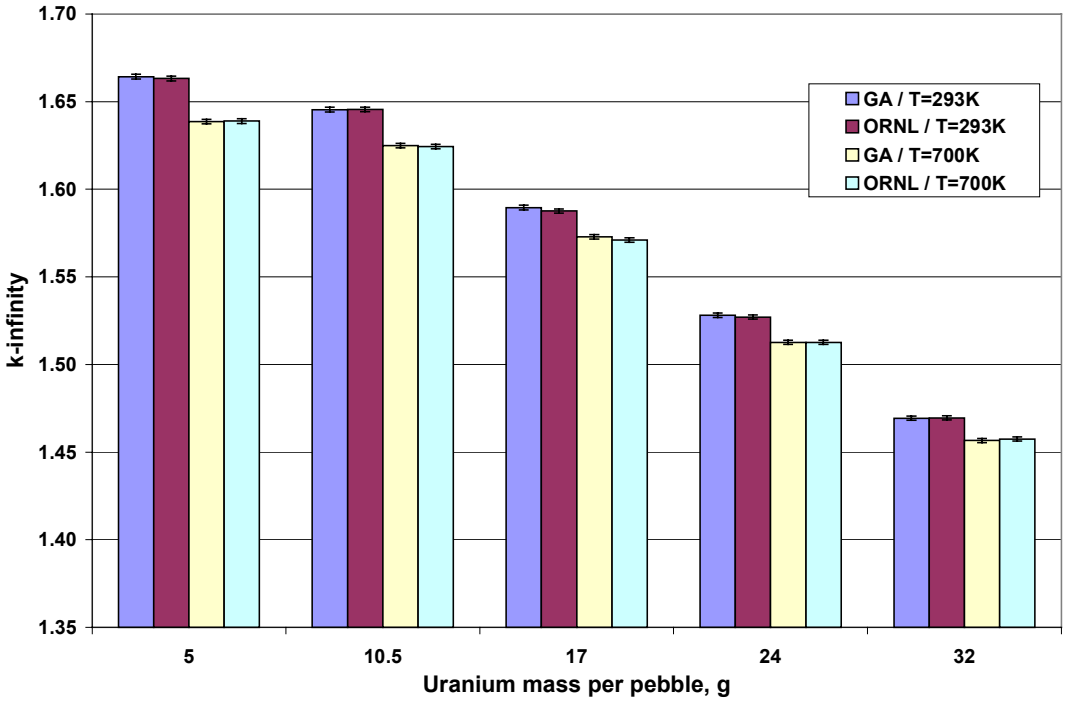

Fig.9 k-infinity as a function of uranium mass per HTR UOX sphere

likewise practical identical effective multiplication factors as seen in Figure 9 (MCNP-4C3 calculations). Also HTR pebble bed systems with PuO_2 as fuel (1 g Pu with different isotopic composition) show no significant difference for keff for the two scattering models.

We interpret these results with the small differences in the total neutron scattering cross sections of the different models and the comparable hard spectra of the analysed systems (compared to spectra in pure graphite).

5. Conclusion

For reactor-grade polycrystalline graphite the neutron-scattering dynamics was re-evaluated considering new proposals from ORNL [10] and NCSU [11] concerning the basic frequency distribution for the scattering law generation. The effect of the basic frequency distribution proposed by ORNL and NCSU on differential and integral neutron cross sections as well as neutron density flux spectra was compared to that of the approved phonon spectrum of GA which was taken for the standard data sets in ENDF/B-VI or JEF-2.2. In our study we have found that temperature dependent phonon spectra derived from measured double-differential neutron cross sections are not suitable to describe all aspects of neutron scattering and neutron thermalisation. So we reported here only of results generated with the theoretical models for $\rho(\omega)$ of ORNL, NCSU and GA. For differential and integral neutron cross sections these models give very good agreement within the published accuracy of measurements. But the Young, Koppel (GA) distribution seems to be slightly more suitable than the ORNL spectrum especially regarding the specific heat in the temperature range from room temperature to some hundred degrees. Discussing the effect for double-differential neutron scattering data one can say that the GA distribution slightly underestimates the quasielastic neutron scattering. But for the inelastic scattering the general agreement is better than with the ORNL model. The NCSU model is comparable to the GA model. For the generation of thermal neutron scattering data it is important to choose a suitable α and β grid, oriented at the frequency distributions. All comparisons made here for the different models are related to thermal neutron scattering data sets generated with the identical processing system (LEAPR-NJOY) and adequate criteria for the chosen α and β grid.

For neutron thermalisation the measured neutron flux density spectra in pure and poisoned graphite are well reproduced by the three frequency distributions. The theoretical spectra agree in neutron temperature but the GA and NCSU data sets give slightly softer spectra. But we do not expect great differences in effective multiplication factor for graphite moderated systems and consequently also not for moderator temperature coefficients of reactivity.

References

1) V. McLane,V. (ed.), "ENDF-102, Data formats and Procedures for the Evaluated Nuclear Data File ENDF-6, " BNL-NCS 44945-01/04, Revision April 2001. Available from http://www.nndc.bnl.gov/nndcscr/documents/endf/endf102/
2) R. E. Mac Farlane; D. W. Muir, "The NJOY Nuclear Data Processing System Version 91," LA-12740 (1994)
3) J. U. Koppel, J. R. Triplett; Y. D. Naliboff, "GASKET, a Unified Code for Thermal Neutron Scattering," GA-7417 (1966) (at IKE modifications of GASKET2)
4) A. Yoshimori, Y.Kitano, "Theory of the Lattice Vibration of Graphite," J. Phys. Soc. Japan **11**, 352 (1956)
5) J. A. Young, J. U. Koppel, "Phonon Spectrum of Graphite," J. Chem.Phys. **42**, 357 (1965)

J. A. Young, N. F. Wikner, D. E. Parks, "Neutron Thermalisation in Graphite II," Nukleonik **7**, 295 (1965)
6) J. U. Koppel, D. H. Houston, "Reference Manual for ENDF Thermal Neutron Scattering Data," GA-8774 (1968); ENDF-269
7) C. Nordborg, M. Salvatores, " Status of the JEF Evaluated Data Library.," Proceedings of International Confererence on Nuclear Data for Science and Technology. Gatlinburg, Tennessee, USA, May 9-13, 1994, Vol. 2, 680 (1994)
"The JEF-2.2 Nuclear Data Library;" NEA Data Bank, JEFF Report 17 (April 2000)
J. Keinert, M.Mattes, "JEF-1 Scattering Law Data," IKE 6-147, JEF Report 2, JEF/DOC 41.2 (1984)
8) R. E. MacFarlane, "New Thermal Neutron Scattering Law Files for ENDF/B-VI, Release 2," LA-12639-MS, ENDF-356 (1994)
9) R. Nicklow, N. Wakabayashi, H. G. Smith, "Lattice Dynamics of Pyrolytic Graphite," Phys. Rev. B **5**, 4951 (1972)
10) F. C. Difilippo, J. P. Renier, A. I. Hawari, "Benchmarks for the Scattering Kermel of Graphite," Proceeding of the PHYSOR 2002: International Conference on the New Frontiers of Nuclear Technology, Seoul, South Korea, 7-10 October (2002)
11) B. Wehring, "Development and Validation of Temperature Dependent Thermal Neutron Scattering Laws for Applications and Safety Implications in Generation IV Reactor Design, " Workshop on Nuclear Data Needs for generation IV Systems, April 2003, JEFF Report 17
12) W. De Sorbo, W. W. Tyler, "The specific heat of graphite from 13 to 300K," J. Chem Phys **21**, 1660 (1953)
13) H. M. Spencer, "Empirical heat capacity equation of gases and graphite," J. Ind. Eng. Chem. **40**, 2152 (1948)
14) W. L. Whittemore, "Neutron Scattering by Reactor-Grade Graphite," Nucl. Sci. Eng. **33**, (1967)
15) F. Carvalho, "Inelastic Scattering of Thermal Neutrons in Graphite," Nucl. Sci. Eng. **34**, 224 (1968)
16) A. Steyerl, W. D. Trüstedt. "Experiments with a Neutron Bottle," ZP **267**, 379 (1974)
17) J. M. Neill, et al., "Integral Neutron Thermalization," GA-6753 (1965)
18) D. J. Hughes, R. B. Schwartz, "Neutron Cross Sections," BNL-325 (1958)
19) C. J. Young, D. Huffman, "Experimental and Theoretical Neutron Spectra," GA-5319 (1964)
20) D. F. Newman, B. F. Gore, "Neutron multiplication factors as a function of temperature: a comparison of calculated and measured values for lattices using $^{233}UO_2$-ThO_2 fuel in graphite," Nucl. Techn**. 37**, 227 (1978)
21) J. C. Kuijper, et al., "HTR-N Plutonium Cell Burnup Benchmark: Definition, Results & Intercomparison," Proceeding of the PHYSOR 2004: International Conference on the Physics of Fuel Cycles and Advanced Nuclear Systems, Chicago, IL, USA, 25-29 April 2004